Chapter 2
Introduction and Basic Theory

2.1 A Classical Mechanical Harmonic Oscillator

The harmonic oscillator is a prominent, basic textbook example of a classical mechanical system. While we do not want to discuss it in great detail as it can be found in any introductory physics textbook (see for example [1]), we would like to briefly review its features and introduce some of the nomenclature that will be used throughout this thesis.

   Mechanical oscillations are a widespread form of motion in nature, for example, it can be found in almost any kind of physical system—from microscopic objects such as molecules up to the biggest found in our universe including neutron stars or more familiarly in systems like clocks, engines or musical instruments. The concept is always the same: an oscillation is the repetitive variation of some parameter around a central value. For example, a system at an initial position x_0 experiences a restoring force F that is proportional to its position x, returns to its point of origin and subsequently moves back to x_0. As long as the system stays decoupled from its environment it continues with this oscillatory movement. According to Newton's second law, the system is described by

$$F = m\ddot{x} = -kx, \tag{2.1}$$

where F is a force, m is the mass of the harmonic oscillator, $\ddot{x}$ is the second derivative of its position with respect to time and k is a positive constant, usually referred to as the spring constant. This is a simple differential equation and one easily sees that the equation of motion is given by

$$x(t) = A \sin(\omega_m t + \varphi). \tag{2.2}$$

Here A is the amplitude, which is determined by the initial conditions and $\omega_m = 2\pi f_m$ is the oscillator's eigenfrequency. The phase φ is the position of the oscillator

relative to the point of origin at $t = 0$ and is also determined by the initial conditions. In fact A and φ are given by [1]

$$A = \sqrt{\frac{\dot{x}^2(0)}{\omega_m} + x^2(0)},\tag{2.3}$$

$$\varphi = \arctan\left(\omega_m \frac{x(0)}{\dot{x}(0)}\right).\tag{2.4}$$

The eigenfrequency of the system is

$$\omega_m = \frac{2\pi}{\tau_m} = \sqrt{\frac{k}{m}},\tag{2.5}$$

with τ_m being the oscillation period. The total energy E_{tot} of the system is conserved and only its kinetic E_k and potential E_p components vary over time

$$E_k(t) = \frac{m}{2}\dot{x}^2 = \frac{k}{2}A^2\cos^2(\omega_m t + \varphi)\tag{2.6}$$

$$E_p(t) = \frac{k}{2}x^2 = \frac{k}{2}A^2\sin^2(\omega_m t + \varphi).\tag{2.7}$$

As a result the total energy is

$$E_{tot} = E_k + E_p = \frac{m}{2}\omega_m^2 A^2.\tag{2.8}$$

Any real harmonic oscillator, however, experiences some kind of friction as it interacts with its environment and therefore we have to include a damping term in the differential equation describing the system:

$$\ddot{x} + \gamma_m\dot{x} + \omega_m^2 x = 0.\tag{2.9}$$

Here γ_m is the damping rate and it determines how fast the oscillation decays. Again, the equation of motion can be easily solved and is given by [1]

$$x(t) = A_d\, e^{-\frac{\gamma_m}{2}t} \sin\left[\sqrt{\omega_m^2 - \left(\frac{\gamma_m}{2}\right)^2}\,t + \varphi_d\right].\tag{2.10}$$

A very useful quantity for a damped harmonic oscillator is its quality factor Q, which is a measure of how many oscillations it undergoes before its amplitude decays by a factor of e:

$$Q := \frac{\omega_m}{\gamma_m}.\tag{2.11}$$

The quality factor determines the behavior of the damped harmonic oscillator and the three different alternatives are:

- $Q > \frac{1}{2}$: The underdamped oscillator is a system that oscillates at a slightly different frequency than the free harmonic oscillator and gradually decays to zero.

- $Q = \frac{1}{2}$: The critically damped oscillator attempts to return to its equilibrium position as quickly as possible and does this without oscillating at all.

- $Q < \frac{1}{2}$: The overdamped oscillator also returns to its equilibrium position without oscillations but takes longer than in the critically damped case—the smaller Q becomes, the longer it takes (Fig. 2.1).

Often harmonic oscillators are not only damped but they are also coupled to an external bath that drives their motion. The differential equation describing such a damped, driven harmonic oscillator reads

$$\ddot{x} + \gamma_m \dot{x} + \omega_m^2 x = \frac{F(t)}{m}, \tag{2.12}$$

where $F(t)$ in the simplest case is a harmonic driving force of the form $F(t) = F_0 \sin(\omega t)$ but can in general take the form of any arbitrary external force. We can again take an Ansatz of the form $x(t) = A \sin(\omega t + \varphi)$ (if we neglect the initial transient behavior of the system [2]) and after some simple calculations we obtain

$$A = \frac{F_0/m}{\sqrt{(\omega_m^2 - \omega^2)^2 + \omega^2 \gamma_m^2}} \tag{2.13}$$

for the amplitude of the motion of the oscillator, while the phase evolves according to

$$\varphi = \arctan \frac{-\omega \gamma_m}{\omega_m^2 - \omega^2}. \tag{2.14}$$
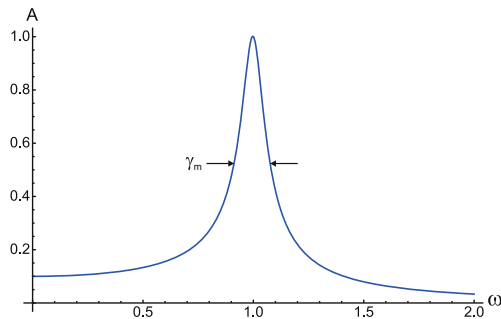
Fig. 2.1 The amplitude response A of a damped, driven harmonic oscillator described by (2.13) as a function of frequency ω. In this example the unperturbed frequency $\omega_m = 1$ and the damping $\gamma_m = 0.1 \cdot \omega_m$, which is defined as the full width at half maximum (FWHM) of the resonance

The response of the damped, driven harmonic oscillator is similar to a Lorentzian and has its resonance close to the natural frequency of the oscillator. It is given by

$$\omega_{res} = \omega_m \sqrt{1 - \frac{\gamma_m^2}{2\omega_m^2}}. \tag{2.15}$$

The general form of $x(t)$ in its Fourier space is [2]

$$\tilde{x}(\omega) = \frac{\tilde{F}(\omega)}{m} \cdot \frac{1}{\omega_m^2 - \omega^2 + i\omega\gamma_m}, \tag{2.16}$$

where $\tilde{F}(\omega)$ is the Fourier transform of an external driving force $F(t)$. For an oscillator subject to Brownian noise, i.e. coupled to a thermal bath at temperature T, the bath can be described as an infinite sum of harmonic oscillators exerting a force of equal amplitude, i.e. $F_{th}(t) = \sum_i F_{ext}^i$. Its power spectrum $S_{xx}(\omega) = \langle \tilde{x}(\omega)\tilde{x}^*(\omega) \rangle$ is given by

$$S_{xx}(\omega) = \frac{\tilde{F}_{th}}{m^2} \cdot \frac{1}{(\omega_m^2 - \omega^2)^2 + \omega^2\gamma_m^2}, \tag{2.17}$$

where $\tilde{F}_{th}$ is constant in frequency for the Brownian bath. Throughout this thesis γ_m is defined as the full width at half maximum (FWHM). The Wiener-Khinchin theorem states that the power spectral density of a wide-sense stationary random process, i.e. a stochastic process with a constant mean (here $x(t)$), is equal to the Fourier transform of its autocorrelation function [3]:

$$S_{xx}(\omega) = \int\limits_{-\infty}^{+\infty} \langle x(t)x^*(t - \tau) \rangle e^{-i\omega\tau} \, d\tau, \tag{2.18}$$

or equivalently for $\tau = 0$

$$\langle x^2 \rangle = \int\limits_{-\infty}^{+\infty} S_{xx}(\omega) \, d\omega = \frac{F_{th}}{m^2} \cdot \frac{\pi}{\omega_m^2 \gamma_m}. \tag{2.19}$$

Here the solution of the integral for Brownian noise is taken from [4], where the integral is done from 0 to ∞ and therefore differs by a factor of 2. This result is very important for this work—it connects the measured power spectrum of a harmonic oscillator to its temperature. This can be seen by using the equipartition theorem: for a 1-dimensional oscillator in thermal equilibrium the total average energy $\langle E \rangle$ is equally distributed between the kinetic E_k and the potential energy E_p of the system

$$\langle E \rangle = \langle E_k \rangle + \langle E_p \rangle = \frac{1}{2} k_B T + \frac{1}{2} k_B T = k_B T, \tag{2.20}$$

where k_B is the Boltzmann constant and T the oscillators temperature. Therefore, using (2.7) and (2.20) we obtain $m \, \omega_m^2 \, \langle x^2 \rangle = k_B T$. Given that (2.19) holds

$$F_{th} = \frac{m \, \gamma_m \cdot k_B T}{\pi}. \tag{2.21}$$

The power spectrum for a damped harmonic oscillator, driven by Brownian noise is finally given by

$$S_{xx}(\omega) = \frac{\gamma_m \cdot k_B T}{\pi \, m} \cdot \frac{1}{(\omega_m^2 - \omega^2)^2 + \omega^2 \gamma_m^2}. \tag{2.22}$$

2.1.1 Normal Modes of Coupled Harmonic Oscillators

An interesting effect occurs if two harmonic oscillators are coupled together (see Fig. 2.2)—for sufficiently strong coupling the two oscillators can be described as one single system oscillating at frequencies that are determined by their coupling strength. The differential equations for two simple harmonic oscillators that are coupled by a spring with spring constant k_j are

$$m\ddot{x}_1 = -kx_1 + k_j(x_2 - x_1),$$
$$m\ddot{x}_2 = -kx_2 + k_j(x_1 - x_2). \tag{2.23}$$
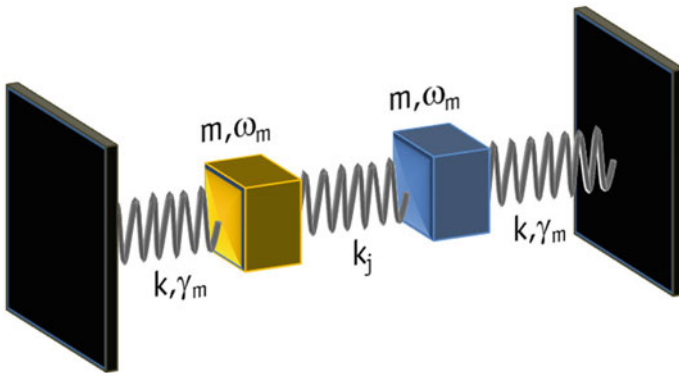
Fig. 2.2 Coupled harmonic oscillators. Two oscillators with masses m and frequencies ω_m are each coupled to an environment via a spring with a spring constant k and a damping rate γ_m. In addition, they are coupled to each other via a joint spring with a spring constant k_j. In Chap. 6 we present an experiment where the two oscillators are a mechanical resonator and an optical field that are strongly coupled to each other

For simplicity, here the oscillators have the same mass m and spring constant k. Taking the Ansatz $x_1(t) = A \sin(\omega t + \varphi)$ and $x_2(t) = B \sin(\omega t + \varphi)$ and substituting into (2.23) we find

$$
\begin{aligned}
(k + k_j - m\omega^2)A - k_j B &= 0, \\
-k_j A + (k + k_j - m\omega^2)B &= 0.
\end{aligned}
\tag{2.24}
$$

For the equation to have a non-trivial solution the determinant of the system of equations must be singular, i.e. zero:

$$
(k + k_j - m\omega^2)^2 - k_j^2 = 0.
\tag{2.25}
$$

This is a simple quadratic equation in ω and assuming that $\omega \geq 0$ we obtain

$$
\omega_1 = \sqrt{\frac{k + 2k_j}{m}},
\tag{2.26}
$$

$$
\omega_2 = \sqrt{\frac{k}{m}}.
\tag{2.27}
$$

Substituting back into (2.24) we find $A = B \equiv A_1$ and $A = -B \equiv A_2$ for the two frequencies, respectively. The most general equations of motions now are

$$
\begin{aligned}
x_1(t) &= A_1 \sin(\omega_1 t + \varphi_1) + A_2 \sin(\omega_2 t + \varphi_2), \\
x_2(t) &= -A_1 \sin(\omega_1 t + \varphi_1) + A_2 \sin(\omega_2 t + \varphi_2).
\end{aligned}
\tag{2.28}
$$

The amplitudes $A_{1,2}$ and the phases $\varphi_{1,2}$ are determined by the initial conditions of $x_{1,2}(0)$ and $\dot{x}_{1,2}(0)$. The motion of the oscillators can therefore be decomposed into two normal modes with frequencies $\omega_{1,2}$ and amplitudes $A_{1,2}$, which are non-degenerate for $k_j \neq 0$. This is true for arbitrarily small k_j as the damping γ_m is zero.

The system becomes even more interesting for two damped (and driven) oscillators. Their uncoupled equations of motions are given by (2.12)

$$
\begin{aligned}
\ddot{x}_1 + \gamma_m \dot{x}_1 + \omega_m^2 x_1 - \frac{k_j}{m}(x_2 - x_1) &= 0, \\
\ddot{x}_2 + \gamma_m \dot{x}_2 + \omega_m^2 x_2 - \frac{k_j}{m}(x_1 - x_2) &= \frac{F(t)}{m}.
\end{aligned}
\tag{2.29}
$$

For simplicity we have assumed that the damping rates γ_m, the masses m and the frequencies ω_m of the oscillators are the same, while only one oscillator is externally driven by a force $F(t)$. These differential equations are solved by (if we neglect the transient terms) [5]

(a)

(b)

(c)
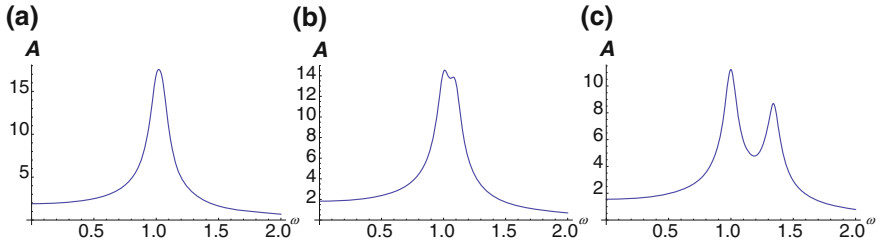
Fig. 2.3 Normal mode splitting of coupled damped harmonic oscillators. The spectrum of two coupled oscillators (Eq. (2.32)) is shown for different coupling constants k_j. The parameters of the oscillators are chosen to be $F(t) = m = k = \omega_m = 1$ and $\gamma_m = 0.1 \cdot \omega_m$. **a** For a coupling $k_j = 0.5 \cdot \gamma_m$ the normal modes are still degenerate, while for $k_j = \gamma_m$ the splitting can already be observed **b**. **c** When increasing the coupling further to $k_j = 4 \cdot \gamma_m$ the modes become very distinct

$$
\begin{aligned}
q_1(t) &= A_1 \sin(\omega t + \varphi_1), \\
q_2(t) &= A_2 \sin(\omega t + \varphi_2),
\end{aligned}
\tag{2.30}
$$

where we have introduced the normal mode coordinates $q_1 = x_1 + x_2$ and $q_2 = x_2 - x_1$. The frequencies of the normal modes are given by

$$
\begin{aligned}
\omega_1 &= \sqrt{\frac{k + 2k_j}{m - \gamma_m^2/4}}, \\
\omega_2 &= \sqrt{\frac{k}{m - \gamma_m^2/4}},
\end{aligned}
\tag{2.31}
$$

and their respective amplitudes

$$
A_i = \frac{F_0/m}{\sqrt{(\omega_i^2 - \omega^2)^2 + \omega^2 \gamma_m^2}},
\tag{2.32}
$$

with $i = 1, 2$. If we now look at the spectrum of the normal modes (Fig. 2.3) we see that the modes are degenerate as long as the coupling strength between the oscillators is small, i.e. $k_j < \gamma_m$. A splitting of the spectrum only occurs if the coupling is stronger than the damping to the environment. In Chap. 6 we use this condition to demonstrate that we enter the strong coupling regime of an optomechanical system.

2.2 A Quantum Mechanical Harmonic Oscillator

In quantum mechanics the harmonic oscillator is one of the simplest examples that is analytically solvable. But already this simple system shows some of the peculiar quantum features that make it so distinct from classical mechanics. The usual starting

point is the classical Hamiltonian function, i.e. the total energy of the system 2.8. If one replaces the classical variables with their corresponding quantum operators, i.e. $x \rightarrow x$ and $m\dot{x} = p \rightarrow -i\hbar\frac{d}{dx}$ one obtains the quantum mechanical Hamiltonian operator

$$H = -\frac{\hbar^2}{2m}\frac{d^2}{dx^2} + \frac{m\omega^2 x^2}{2},$$ (2.33)

with $\hbar$ being the reduced Planck constant. One can rewrite the operators x and p in terms of the creation $a^\dagger$ and annihilation a operators

$$x = \sqrt{\frac{\hbar}{2m\omega}}(a + a^\dagger),$$

$$p = \sqrt{\frac{m\omega\hbar}{2}}(a - a^\dagger).$$ (2.34)

As x and p fulfill the commutation relation $[x, p] = i\hbar$, a and $a^\dagger$ obey the following relations

$$[a, a^\dagger] = 1 \text{ and } [a, a] = [a^\dagger, a^\dagger] = 0.$$ (2.35)

Hence the Hamiltonian can be expressed as

$$H = \hbar\omega\left(a^\dagger a + \frac{1}{2}\right),$$ (2.36)

and the corresponding Schrödinger equation reads

$$a^\dagger a \, \psi = \left(\frac{E}{\hbar\omega} - \frac{1}{2}\right)\psi.$$ (2.37)

This is an eigenvalue equation for the so-called number operator $a^\dagger a$, which obeys the commutation relations $\left[a^\dagger a, a^\dagger\right] = a^\dagger$ and $\left[a^\dagger a, a\right] = -a$. The eigenfunctions of the eigenvalue equation are solutions of the Schrödinger equation. The lowest eigenfunction ψ_0 is the ground state of the harmonic oscillator, which we can calculate using $a \, \psi_0 = 0$

$$\psi_0(x) = \left(\frac{m\omega}{2\hbar}\right)^{1/4} \exp\left(-\frac{m\omega}{2\hbar}x^2\right).$$ (2.38)

The eigenfunction for the nth energy eigenstate then is

$$\psi_n(x) = \sqrt{\frac{1}{n!}}(a^\dagger)^n \psi_0(x).$$ (2.39)

It is now easy to find the energy spectrum for the harmonic oscillator by simply writing down the eigenvalue equation for the Hamiltonian defined in Eq. (2.36), which is discrete and the energy levels are equidistant:

$$E_n = \hbar\omega \left(n + \frac{1}{2} \right). \tag{2.40}$$

We can now also calculate the expectation value for the position operator x and the position operator squared x^2 and find

$$\langle x \rangle = \langle \psi_n | x | \psi_n \rangle = 0, \tag{2.41}$$

$$\langle x^2 \rangle = \langle \psi_n | x^2 | \psi_n \rangle = \frac{\hbar}{m\omega} \left(n + \frac{1}{2} \right). \tag{2.42}$$

The ground state of a quantum mechanical oscillator therefore has non-zero energy and an associated extension

$$E_0 = \frac{1}{2}\hbar\omega,$$

$$x_{zp} = \sqrt{\langle x^2 \rangle_0 - \langle x \rangle_0^2} = \sqrt{\frac{\hbar}{2m\omega}}. \tag{2.43}$$

This so-called zero-point energy is the minimal energy compatible with the Heisenberg uncertainty principle. Another widely used definition of the zero-point extension is the half width at half maximum of the associated wavepacket (2.38) of the oscillator, which differs by a factor $\sqrt{2}$ from how x_{zp} is defined here.

2.2.1 Quantum States

The quantum state that most closely resembles a classical harmonic oscillator is the so-called coherent state, which was first described by Schrödinger in 1926 [6], while the term itself was introduced by Glauber [7]. It is defined as

$$|\alpha\rangle = e^{-\frac{1}{2}|\alpha|^2} \sum_{n=0}^{\infty} \frac{\alpha^n}{\sqrt{n!}} |n\rangle, \tag{2.44}$$

where $|n\rangle$ are the number or Fock states and the average occupation number of the state is given by $\bar{n} = |\alpha|^2$. The variance then is $\Delta n = \sqrt{\bar{n}} = |\alpha|$. The probability $P_\alpha(n)$ of finding an oscillator described by the coherent state in its nth state is given by a Poissonian distribution

$$P_\alpha(n) = e^{-|\alpha|^2} \frac{|\alpha|^{2n}}{n!}. \tag{2.45}$$

Often the coherent state is also defined as a displaced vacuum state [7]

$$|\alpha\rangle = D(\alpha)|0\rangle, \tag{2.46}$$

where $|0\rangle$ is the vacuum state and $D(\alpha) = \exp(\alpha a^\dagger - \alpha^* a)$ the displacement operator. As $D(\alpha)$ is unitary, it is relatively easy to see (cf. [7]) that the coherent state is an eigenfunction of the annihilation operator, i.e. $a|\alpha\rangle = \alpha|\alpha\rangle$. The output field of a laser, for example, is well described by a coherent state. The phase of such a coherent state has an uncertainty of $\Delta\phi = 1/2\sqrt{\bar{n}}$ (see e.g. [3]) for $\alpha \gg 1$ and hence the coherent state obeys the uncertainty relation $\Delta\phi \cdot \Delta n = \frac{1}{2}$. In other words, the coherent state has an equally spread uncertainty in phase-space with a width of 1/2. It approaches the case of a classical oscillator that has no uncertainty with increasing α as the uncertainty becomes less significant.

A harmonic oscillator in thermal equilibrium with a bath at temperature T must be described as a mixture of pure states, i.e. it is in a thermal state (see for example [8])

$$\rho = \sum_{n=0}^{\infty} \frac{\bar{n}^n}{(1+\bar{n})^{n+1}} |n\rangle\langle n|, \tag{2.47}$$

where $\bar{n} = (\exp\{\hbar\omega/k_B T\} - 1)^{-1}$ is the oscillator's mean occupation number following the Bose-Einstein statistics. In the large temperature limit, i.e. $k_B T \gg \hbar\omega$, the mean thermal occupation $\bar{n}$ due the equipartition of energies is

$$\bar{n} \approx \frac{k_B T}{\hbar\omega} - \frac{1}{2}. \tag{2.48}$$

Only close to the ground state, i.e. for $\bar{n} = \mathcal{O}(1)$, this approximation does not hold and one has to use the full Bose-Einstein statistics. Here we have used the density matrix representation of the state in the Fock basis, which is defined as

$$\rho = \sum_{m,n} c_{m,n} |m\rangle\langle n|, \tag{2.49}$$

with $c_{m,n} = \langle m|\rho|n\rangle$.

2.2.2 Phase-Space Distribution

A classical particle has well defined position x and momentum p. For an ensemble of such particles one can define a probability distribution, which gives the probability of finding a particle for a given x and p in phase space. In the quantum domain there is no exact analogue due to the Heisenberg uncertainty principle, but nonetheless a quasi-probability distribution can be defined, the Wigner function [9]. If one takes

the marginal of the Wigner function, i.e. the projection onto the vertical plane defined by for example the x-axis, one recovers the distribution obtained by measurements of (in this example) the x-quadrature of an ensemble of equally prepared quantum systems. This is completely analogous to the classical case. The Wigner function has many properties of a classical probability distribution, e.g. it is real and normalized. However, it can also have negative values, which is the reason why it is called a quasi-probabilistic distribution. The negativity is often taken to determine whether a state is non-classical or not—while this is a sufficient condition, it is not a necessary one. Often states that have a fully positive Wigner distribution, such as the vacuum state or a squeezed coherent state (in fact this is the case for all Gaussian states), are still considered to be quantum (for a more detailed discussion see for example [10]). The Wigner function is defined as [11]

$$W(x, p) = \frac{1}{\pi \hbar} \int_{-\infty}^{+\infty} e^{2ipy/\hbar} \langle x - y | \rho | x + y \rangle dy, \qquad (2.50)$$

where ρ is the density matrix of a general mixed state. The marginals for example for x and p are

$$\int_{-\infty}^{+\infty} dx \, W(x, p) = \langle x | \rho | x \rangle = |\psi(x)|^2,$$

$$\int_{-\infty}^{+\infty} dp \, W(x, p) = \langle p | \rho | p \rangle. \qquad (2.51)$$

And as it is normalized $\int dx \int dp \, W(x, p) = \text{Tr}(\rho) = 1$, where Tr is the trace. The Wigner function for the thermal state (2.49) and a squeezed coherent state are shown in Fig. 2.4. More details on Wigner functions can be found in [4].
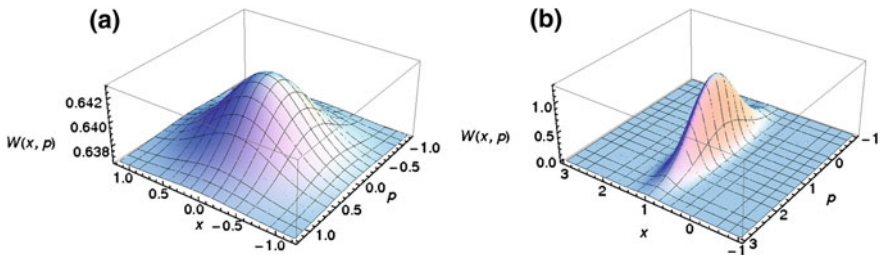

Fig. 2.4 **a** shows the Wigner function $W(x, p)$ of a thermal state. The state has no phase and its mean occupation $\bar{n}$ follows the Bose-Einstein statistics. **b** in contrast, is the Wigner function of a squeezed coherent state, where squeezing of approximately 6 dB in the x-quadrature is shown. All axes are in arbitrary units

2.3 Radiation Pressure

Radiation-pressure effects, i.e. forces acting solely due to the momentum of light, have been discussed as early as the seventeenth century when Johannes Kepler suspected that the inclination of the tails of comets could be due to a mechanical force exerted by the sun [12, 13]. In fact, the tails of a comet are due to the solar radiation that vaporizes particles on the surface of the comet. Radiation pressure from the sun then exerts a force on the coma of the comet (white tail), while the force of the solar wind creates the ionized (blue) tail. In the early twentieth century, experiments by Lebedev [14] and Nichols and Hull [15] first verified unambiguously predictions by Maxwell [16] and Bartoli [17] on the strength of the radiation-pressure force.

In the 1960s and 70s, Braginsky and colleagues studied radiation-pressure effects in the context of gravitational wave antennae—they experimentally and theoretically analyzed the sensitivity limits due to the quantum nature of light [18, 19]. Braginsky also predicted that the radiation pressure inside a cavity with finite decay time would give rise to dynamic backaction, the underlying mechanism to the parametric instabilities and cooling of a mechanical oscillator, which will be discussed later in this section [20]. In the 1980s, also Caves [21] and Meystre et al. [22] analyzed the radiation-pressure noise in interferometers. First experiments on radiation-pressure effects in cavities with macroscopic mechanical oscillators were performed in the 1980s [23]. Subsequently, several theoretical proposals for quantum optics experiments in a cavity using radiation-pressure effects were published, such as the generation of squeezed light [24, 25], quantum non-demolition measurements of photon numbers [26, 27], feedback-cooling of the mechanical motion [28] (which was experimentally realized in [29]), entanglement between the optical and the mechanical mode [30–32], and the quantum-state transfer from the light field to the mechanical oscillator [33]. However, first experiments were only realized in recent years (except for [23]): measurements of the motion of a mechanical oscillator [34–36], parametric amplification of the mechanical motion [37], cavity cooling of the mechanical resonator [38–41], cryogenic cavity cooling [42–45] and strongly coupled optomechanics [46, 47]. For a more detailed historic overview of radiation-pressure forces up to the early twentieth century see [14, 48] and for the more recent developments see for example [49–54]. It is important to note that experiments involving nanomechanical oscillators and microwave cavities have achieved similar results [55–59]. And very recently, the first experimental observation of the quantization of mechanical motion in an optomechanical system was demonstrated [60]. In experiments involving mechanics and qubits [61], as well as microscopic mechanical oscillators quantum effects have also been observed [62].

The system studied throughout this thesis is a Fabry-Pérot cavity, in which one of the end-mirrors is suspended, i.e. it can be described as a damped harmonic oscillator with a resonance frequency ω_m and a mass m, subject to an external thermal bath and coupled to the light inside the cavity via the radiation-pressure force (Fig. 2.5). The interaction between the mechanical and the optical system can be understood qualitatively as follows: light with a wavelength λ impinges on the moving mirror
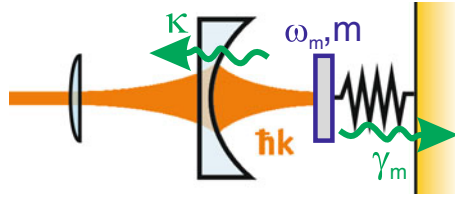
Fig. 2.5 Sketch of the radiation-pressure interaction: light is coupled through a rigid input mirror into an optical resonator with a movable back-mirror of frequency ω_m and mass m. The photons inside the cavity each transfer momentum of $2\hbar k$ onto the movable mirror, displace it and hence acquire a phase shift, depending on its position. The intensity of the light field inside the cavity strongly depends on the relative distance between the mirrors, as well as on their reflectivities—the amplitude cavity decay rate is given by κ. The movable mirror couples to its environment at a rate γ_m

and each photon transfers momentum of $2\hbar k$ onto the mechanics, where $k = 2\pi/\lambda$ is the wavenumber of the light. A quasi-static displacement of the mirror due to the light force changes the length of the cavity and hence the phase of the light field. In a cavity detuned from resonance, the sensitivity of the intra-cavity intensity strongly depends on the length of the cavity and even the typically very small displacement of the suspended end-mirror can modify the light fields' amplitude and phase significantly (see Sect. 3.2.1 for details). In turn, the mechanical displacement is modified by the momentum transfer of the radiation-pressure force. This interaction hence generates an intensity dependent phase shift of the light incident onto the cavity, which is equivalent to the optical or AC Kerr effect [63]. Also, the frequency of the photons hitting the mirrors is changed due to a Doppler-shift from the oscillating mirror, resulting in frequency sidebands in the optical field that are spaced by ω_m.

The radiation-pressure interaction can now be exploited to modify the dynamics of the mechanical oscillator, which is described in detail in the following subsections. One particularly interesting effect is the possibility to damp, i.e. cool, the mechanical motion with the help of the radiation-pressure force. In a very intuitive picture, in close analogy to the sideband cooling of atoms [64], the sidebands in the light field are created due to an energy exchange between the optical and the mechanical mode, where the creation of a photon at the frequency $\omega_c + \omega_m$ (ω_c is the cavity frequency) results in the annihilation of a phonon in the mechanical oscillator, while the optical sideband at $\omega_c - \omega_m$ comes from the creation of a phonon. If we now detune the cavity resonance with respect to the incoming laser, or vice versa, an imbalance between the two first-order sidebands is created resulting in an effective cooling of the mechanical mode or a net heating, depending on the sign of the detuning (cf. Fig. 2.6). The latter case also gives rise to entanglement between the optical and the mechanical mode, a true optomechanical feature. The detailed physical mechanisms behind the cooling, the entanglement and the modification of the dynamics in general, both in a classical and a quantum framework, are derived in the following sections.
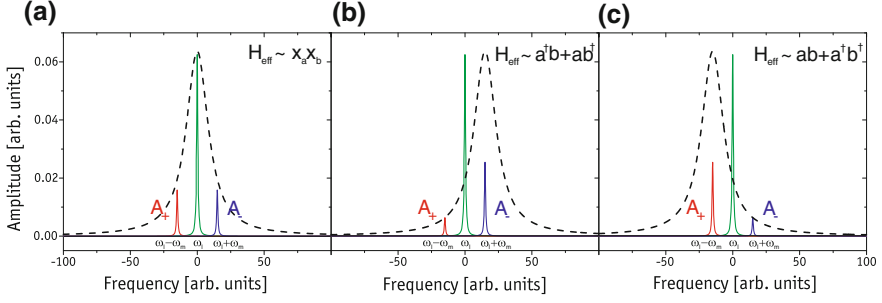
Fig. 2.6 **a** A laser field (*green*) with frequency ω_l drives the optomechanical cavity (*dashed black line*) on resonance. Due to the radiation-pressure interaction frequency sidebands are created at $\omega_l - \omega_m$ (*red*) and $\omega_l + \omega_m$ (*blue*) with rates $A_\pm$, respectively, given by Eq. (2.72). The rates $A_\pm$ are equal and this configuration allows for example to perform quantum non-demolition measurements as proposed in [26, 27]. **b** The situation becomes quite different if the cavity is detuned with respect to the laser by $\Delta = \omega_m$. The rates become unbalanced and $A_- > A_+$, which results in cooling of the mechanical mode. This can be intuitively understood as the sideband with higher energy (which is created by extracting phonons from the mechanical resonator), the anti-Stokes sideband, becomes stronger than the lower energy Stokes sideband. The corresponding effective interaction Hamiltonian is $\propto a^\dagger b + a b^\dagger$ (see Sect. 2.3.3). **c** When detuning the cavity by $\Delta = -\omega_m$ the effective interaction Hamiltonian becomes a two-mode squeezer, i.e. is $\propto ab + a^\dagger b^\dagger$, which can be used for creating optomechanical entanglement (see Sect. 2.3.6 and Chap. 7). The effective interactions in **b** and **c** are valid in the rotating wave approximation (RWA), i.e. for weak coupling and sideband resolved operation ($\omega_m > \kappa$)

2.3.1 Classical Analysis

The radiation-pressure force F_{rp} inside a Fabry-Pérot cavity is proportional to the intra-cavity light intensity I (see Sect. 3.2.1), which in turn is a function of the length of the cavity (and of the detuning of the laser with respect to the cavity resonance) and hence $F_{rp} = F_{rp}(x)$. If a damped harmonic oscillator is now not only driven by Brownian noise but in addition by an external radiation-pressure force, the differential Eq. (2.12) is modified to

$$\ddot{x} + \gamma_m \dot{x} + \omega_m^2 x = \frac{F_{th}(t) + F_{rp}(x(t))}{m}. \tag{2.52}$$

The equation of motion for such an oscillator in thermal equilibrium can be expressed in terms of its susceptibility, which is simply the response of the system to an applied force, i.e. $\chi(\omega) = \tilde{x}(\omega)/F(\omega)$, or for our case

$$\tilde{x}(\omega) = \chi(\omega) \left(\tilde{F}_{th} + \tilde{F}_{rp}(\omega) \right). \tag{2.53}$$

For a damped harmonic oscillator driven by Brownian noise we know from (2.16) that the susceptibility is given by

$$\chi(\omega) = \frac{1}{m \cdot (\omega_m^2 - \omega^2 + i\omega\,\gamma_m)}. \tag{2.54}$$

The radiation-pressure force modifies the dynamics of the oscillator and therefore the susceptibility can be rewritten as an effective susceptibility, with an effective frequency ω_{eff} and an effective oscillator damping γ_{eff}

$$\chi_{eff}(\omega) = \frac{1}{m \cdot (\omega_{eff}^2 - \omega^2 + i\omega\,\gamma_{eff})}, \tag{2.55}$$

where, in the limit of $Q \gg 1$, the modified frequency and damping rate are given by [39]

$$\omega_{eff}(\omega) = \omega_m \left(1 + M \cdot \left[1 - \frac{\omega^2 + \Delta_0^2}{\kappa^2}\right]^{-1}\right), \tag{2.56}$$

$$\gamma_{eff}(\omega) = \gamma_m \left(1 + M \cdot \frac{Q\kappa}{\omega}\right). \tag{2.57}$$

Here $M = \frac{4\pi\Delta_0 \cdot I}{\lambda \cdot \kappa^2 \cdot L \cdot m\omega_m^2}$ and $\kappa = \frac{\pi c}{2L \cdot F}$ is the cavity amplitude decay rate, with L being the cavity length, c the speed of light and F the finesse, while $\Delta_0 = \omega_c - \omega_l$ is the cavity detuning (modulo $[2\pi \cdot FSR]$), with the free spectral range $FSR = c/2L$ and the laser frequency ω_l. The dynamics can be modified by choosing the sign of the detuning, which will be explained in more detail later. We can now write down the spectral response of the oscillator

$$S_{xx}(\omega) = \frac{\gamma_m \cdot k_B T}{\pi\,m} \cdot \frac{1}{(\omega_{eff}^2 - \omega^2)^2 + \omega^2\gamma_{eff}^2}. \tag{2.58}$$

It is interesting to note that the radiation-pressure force is completely contained in the effective frequency and damping rate and that only the Brownian noise force appears in the equation of motion $\tilde{x}(\omega)$. According to the fluctuation-dissipation theorem the coupling to the thermal bath at temperature T is uniquely described by γ_m [3, 65]. In analogy to the damped harmonic oscillator subject to a thermal Brownian driving force we use the Wiener-Khinchin theorem and find

$$m\omega_{eff}^2 \langle x^2 \rangle = m\omega_{eff}^2 \int\limits_{-\infty}^{+\infty} \tilde{x}(\omega)d\omega = k_B T \cdot \frac{\gamma_m}{\gamma_{eff}} = k_B T_{eff}, \tag{2.59}$$

here we have introduced an effective temperature $T_{eff} = T\frac{\gamma_m}{\gamma_{eff}}$, which again satisfies the equipartition theorem for the harmonic oscillator. For an experiment where the parameters are chosen such that γ_{eff} is increased, the radiation-pressure interaction allows for cooling of the mechanical mode.

In our optomechanical system the mass in the radiation-pressure interaction is not the actual mass m of the oscillating mirror but rather a quantity that takes the finite overlap of the optical and the mechanical mode into account, the effective mass m_{eff}. An extensive theoretical analysis of the matter can be found in [66], while the experimental procedure to determine the effective mass is described in Sect. 3.10.

2.3.2 Quantum Analysis

In this section we will analyze the radiation-pressure interaction between an optical cavity mode and a mechanical oscillator in a quantum framework. The derivation closely follows [67, 68] and assumes that we detect a single mechanical mode only, that the individual mechanical modes do not couple to each other and that we only have to consider a single cavity mode, i.e. $\omega_m \ll c/2L$. The full Hamiltonian of the system at hand is [69]

$$H = \hbar\omega_c\, a^\dagger a \,+\, \frac{1}{2}\hbar\omega_m \left(p_m^2 \,+\, x_m^2\right) - \hbar g_0 a^\dagger a x_m + i\hbar E \left(a^\dagger e^{-i\omega_l t} - a e^{i\omega_l t}\right). \tag{2.60}$$

Here ω_c is the cavity frequency, a and $a^\dagger$ are the annihilation and creation operators of the cavity field, with $[a, a^\dagger] = 1$, p_m and x_m are the dimensionless versions of the momentum and position operators of the mechanical oscillator defined in Eq. (2.34), i.e. $[x_m, p_m] = i$ and their creation and annihilation operators are b and $b^\dagger$, respectively, g_0 is the frequency shift of the cavity due to the displacement of the mechanical oscillator by a single-photon, E related to the input laser power P by $|E| = \sqrt{2P\kappa/\hbar\omega_l}$ and ω_l the laser frequency. The optomechanical coupling rate g_0 is a measure for the frequency shift of the cavity when the mechanics is displaced by x_{zp} and is defined as $g_0 = \frac{\partial\omega_c}{\partial x} \cdot x_{zp}$. For a Fabry-Pérot cavity g_0 is given by

$$g_0 = \frac{\omega_c}{L} \sqrt{\frac{\hbar}{m_{eff} \cdot \omega_m}}, \tag{2.61}$$

as $\omega_c = \frac{2\pi c}{\lambda} = \frac{2\pi c \cdot n}{L}$, with $n \in \mathbb{N}$, where L is the cavity length. The first term of the Hamiltonian is the energy of the cavity field, while the second term is the corresponding quantity for the mechanical mode. The third term is the optomechanical interaction Hamiltonian H_{rp} on which we will concentrate in the following and the last term describes the coupling of the laser to the cavity mode.

In order to obtain the dynamics of the optomechanical system, one usually finds the Langevin equations of the system—they are stochastic differential equations describing the time evolution of a subset of degrees of freedom, where the mean value of the system slowly varies and is treated dynamically, while the small fluctuations around the mean value are treated probabilistically. Paul Langevin initially considered the Brownian motion of particles [70] and assumed that such a particle

is subject to a systematic force, i.e. a viscous drag, and a rapidly fluctuating force, which comes from surrounding particles randomly impacting on the system under investigation with a mean amplitude of zero, i.e. the net force is zero on average. He treated this rapid force statistically, assuming that it was independent from the viscous drag and arrived at an expression for the mean motion of the particle (for an introduction to Langevin equations see for example [71]). In general, the Langevin equations for an operator $\hat{O}$ are given by $\partial \hat{O}/\partial t = (i/\hbar)\left[H, \hat{O}\right] + \hat{N}$, where $\hat{N}$ is the corresponding noise operator of $\hat{O}$. The quantum Langevin equations for the optomechanical system therefore are

$$
\begin{aligned}
\dot{x}_m &= \omega_m p_m, \\
\dot{p}_m &= -\omega_m x_m - \gamma_m p_m + g_0\, a^\dagger a + \xi, \\
\dot{a} &= -(\kappa + i\Delta_0)\, a + i g_0\, a\, x_m + E + \sqrt{2\kappa}\, a^{in},
\end{aligned}
\tag{2.62}
$$

where γ_m is the damping of the viscous force that acts on the mechanical mode and ξ is the Brownian stochastic force with zero mean amplitude. We have also introduced the cavity detuning $\Delta_0 = \omega_c - \omega_l$ and the optical vacuum input noise a^{in}. In order to simplify the problem we can take a semi-classical approach by assuming a strong intra-cavity field amplitude $|\alpha_s| \gg 1$, which allows us to write down a steady state amplitude for each operator with small zero-mean fluctuations, i.e. for the generic operator $\hat{O} = \hat{O}_s + \delta\hat{O}$, where $\hat{O}_s$ now is the mean value with the fluctuation operator $\delta\hat{O}$. We first find the steady state values by setting the time derivatives in (2.62) to zero

$$
x_s = \frac{g_0 |\alpha_s|^2}{\omega_m},
\tag{2.63}
$$

$$
\alpha_s = \frac{E}{\kappa + i\Delta}.
\tag{2.64}
$$

Due to the bright light field inside the cavity the mechanical oscillator is displaced by $x'_s = x_s \cdot x_{zp}$ into a new equilibrium position. Here Δ is the detuning of the cavity including radiation-pressure effects

$$
\Delta = \Delta_0 - \frac{g_0^2 |\alpha_s|^2}{\omega_m}.
\tag{2.65}
$$

The nonlinear equation for Δ can be solved analytically but gives a rather lengthy expression which will not be shown here.[1] The Langevin equations can now be rewritten for the fluctuation operators, while neglecting their higher order terms:

---

[1] Note that the detuning of the laser to the cavity in an experiment equals the detuning for an empty cavity, if the laser frequency is kept on resonance with the cavity and only part of it is detuned and used for radiation-pressure coupling, i.e. $\Delta = \Delta_0$ for our experimental situation (cf. Chaps. 5 and 6). This of course does not imply $\frac{g_0^2 |\alpha_s|^2}{\omega_m} = 0$ in (2.65).

$$\delta \dot{x}_m = \omega_m \delta p_m,$$
$$\delta \dot{p}_m = -\omega_m \delta x_m - \gamma_m \delta p_m + g \delta X + \xi,$$
$$\delta \dot{X} = -\kappa \delta X + \Delta \delta Y + \sqrt{2\kappa} X^{in},$$
$$\delta \dot{Y} = -\kappa \delta Y - \Delta \delta X + g \delta x_m + \sqrt{2\kappa} Y^{in}. \tag{2.66}$$

We have introduced the cavity field quadratures $\delta X = \left(\delta a + \delta a^{\dagger}\right)/\sqrt{2}$ and $\delta Y = \left(\delta a - \delta a^{\dagger}\right)/i\sqrt{2}$, as well as the corresponding Hermitian input noise operators $X^{in} = \left(a^{in} + a^{in,\dagger}\right)/\sqrt{2}$ and $Y^{in} = \left(a^{in} - a^{in,\dagger}\right)/i\sqrt{2}$. The effective optomechanical coupling rate in the linearized quantum Langevin equations is

$$g = \alpha_s \cdot g_0 = \frac{2\omega_c}{L} \sqrt{\frac{P\kappa}{m_{eff}\omega_m\omega_l\left(\kappa^2 + \Delta^2\right)}}. \tag{2.67}$$

In an actual experiment the cavity is never perfectly single-sided, i.e. it is not possible for a mirror to have unity reflectivity, and therefore leakage of the field through the second mirror needs to be taken into account

$$g = \frac{2\omega_c}{L} \sqrt{\frac{P\kappa'}{m_{eff}\omega_m\omega_l\left((\kappa' + \bar{\kappa})^2 + \Delta^2\right)}}, \tag{2.68}$$

where we have introduced the amplitude cavity decay rate for the first κ' and the second mirror $\bar{\kappa}$. They are defined as $\kappa_i = \frac{c}{4L} \cdot \varrho_i$, where ϱ_i are the losses associated with the respective mirror and $\kappa = \sum_i \kappa_i$.

By linearizing the problem we have lost the non-linear interaction character in Eq. (2.60), which would be accessible for example by single photons. However, we have gained significantly in the achievable interaction strength by simply increasing the intra-cavity field. When solving the linearized Langevin equations according to [67, 68] we finally obtain the effective susceptibility for the mechanical oscillator interacting with the cavity mode via radiation pressure

$$\chi_{eff}(\omega) = \frac{\omega_m}{\omega_m^2 - \omega^2 - i\omega\gamma_m - \frac{g^2\Delta\omega_m}{(\kappa - i\omega)^2 + \Delta^2}}. \tag{2.69}$$

The effective mechanical frequency and damping rate are given by

$$\omega_{eff}(\omega) = \left(\omega_m^2 - \frac{2\,g^2\Delta\,\omega_m\left(\kappa^2 - \omega^2 + \Delta^2\right)}{\left[\kappa^2 + (\omega - \Delta)^2\right]\left[\kappa^2 + (\omega + \Delta)^2\right]}\right)^{1/2}, \tag{2.70}$$

$$\gamma_{eff}(\omega) = \gamma_m + \frac{g^2\Delta\,\omega_m\kappa}{\left[\kappa^2 + (\omega - \Delta)^2\right]\left[\kappa^2 + (\omega + \Delta)^2\right]}. \tag{2.71}$$

The modification of the mechanical oscillation frequency is called the optical spring effect, as the spring constant of the resonator is effectively modified. This effect has first been observed experimentally in [72] and subsequently been confirmed in several experiments [73–75]. In extreme cases this effect can change the resonance frequency by almost two orders of magnitude [76]. The change in the damping rate can be used to heat or cool the mechanical resonator—when choosing the detuning Δ between the laser and the cavity to be negative the mechanical system is excited by radiation pressure and therefore parametrically driven [37]. However, if $\Delta > 0$ the mechanical motion is damped, which corresponds to an effective cooling of the mode as long as the laser noise is small compared to the thermal noise [77, 78]. The thermal mean occupation of such a damped oscillator is given by the Bose-Einstein statistics $\bar{n} = \left(\exp\left\{ \hbar\omega_m / k_B T_{eff} \right\} - 1 \right)^{-1}$, where the temperature now is an effective mode temperature T_{eff}. It has been theoretically shown that this technique in principle allows for cooling the mechanical mode into its quantum ground state if operating in the sideband-resolved regime, i.e. $\omega_m > \kappa$ [68, 79, 80]. The first experimental demonstrations of such a passive mechanical cavity-cooling have been realized by [38–41, 81], with similar experiments in the microwave regime [55, 57, 58], and recently ground state cooling has been experimentally demonstrated using this technique, both in the optical [82] and the microwave regime [83]. Another interesting quantity for such cooling experiments is the scattering rate $A_\pm$ of laser photons into the Stokes $(+)$ and anti-Stokes $(-)$ sideband, where for positive detuning an imbalance between the sidebands of the form $A_- > A_+$ results in the desired cooling

$$A_\pm = \frac{g^2 \kappa}{8 \left[\kappa^2 + (\Delta \pm \omega_m)^2 \right]}. \tag{2.72}$$

2.3.3 Quantum Opto-Mechanics

The Hamiltonian (2.60) can be rewritten in the interaction picture, i.e. we make a basis change into the frame rotating at the laser frequency ω_l. The corresponding unitary transformation is $U(t) = \exp\left(i\omega_l t a^\dagger a \right)$ and we can first transform the Schrödinger equation

$$i\hbar \frac{d}{dt} |\psi\rangle = H|\psi\rangle \rightarrow i\hbar \frac{d}{dt}\left(U^\dagger |\tilde{\psi}\rangle \right) = HU^\dagger |\tilde{\psi}\rangle, \tag{2.73}$$

where $|\tilde{\psi}\rangle = U|\psi\rangle$. After some simple algebra we get $i\hbar \frac{d}{dt}|\tilde{\psi}\rangle = \tilde{H}|\tilde{\psi}\rangle$, with

$$\tilde{H} = U\left(H - i\hbar\frac{d}{dt} \right) U^\dagger$$

$$= \hbar\Delta a^\dagger a + \frac{1}{2}\hbar\omega_m(p_m^2 + x_m^2) - \hbar g_0 a^\dagger a x_m + \hbar E(a^\dagger + a). \tag{2.74}$$

Another way of qualitatively describing the cooling is to analyze the interaction term H_{rp} of the Hamiltonian. By assuming $\alpha_s \gg 1$ one can write $a \to \alpha_s + a$, where a now is the associated fluctuation operator and $a^\dagger \to \alpha_s + a^\dagger$. By factorizing H_{rp} and neglecting higher order terms in the fluctuation operators we obtain

$$H_{rp} \approx \hbar \alpha_s g_0 (a + a^\dagger) \cdot (b + b^\dagger), \tag{2.75}$$

where we have used the definition for x_m and omitted a static mirror displacement of $\mathcal{O}(\alpha^2 x_m)$, which is defined by (2.63). If we go into another rotating frame by using the unitary operator $U'(t) = \exp\left(i(\Delta a^\dagger a + \omega_m b^\dagger b)t\right)$ we obtain for the linearized interaction Hamiltonian

$$\begin{aligned}
\tilde{H}'_{rp} &= \hbar g (a e^{-i\Delta t} + a^\dagger e^{i\Delta t}) \cdot (b e^{-i\omega_m t} + b^\dagger e^{i\omega_m t}) \\
&= \hbar g (ab\, e^{-i(\Delta+\omega_m)t} + a^\dagger b^\dagger e^{i(\Delta+\omega_m)t}) \\
&\quad + \hbar g (a^\dagger b\, e^{i(\Delta-\omega_m)t} + ab^\dagger e^{-i(\Delta-\omega_m)t}).
\end{aligned} \tag{2.76}$$

The first term is $\propto ab + a^\dagger b^\dagger$, which is a two-mode squeezing (TMS) operation and hence can be used to entangle the optical with the mechanical mode (see Sect. 2.3.6). The second term $\propto a^\dagger b + ab^\dagger$ in turn is simply a beamsplitter (BS) interaction, which results in the cooling described above. If the detuning Δ is chosen to be $+\omega_m$ the phase of the BS vanishes, while the TMS oscillates at a frequency of $2\omega_m$. By performing a perturbation expansion we can see that for this case the TMS term only contributes on the order of $\frac{g}{\omega_m}$ and the BS dominates for small g and sideband resolution ($\omega_m > \kappa$), which corresponds to the so-called rotating wave approximation (RWA). The inverse is true for $\Delta = -\omega_m$.

2.3.4 SQL + Backaction

Due to the quantum nature of light, measurements of the motion of a mechanical oscillator as described in this thesis are fundamentally limited in sensitivity. In general, the uncertainty principle poses a limit on how well one can continuously measure a certain quantity. The phase and the photon number (amplitude) of a light field, for example, are connected by the uncertainty relation $\Delta\phi \cdot \Delta n \geq 1/2$ (for a coherent state this actually becomes an equality if α is large, as shown in Sect. 2.2.1). In order to determine the displacement of the mechanical oscillator we measure the phase shift the movement imparts on a probing light field. The field itself however has a phase uncertainty of $\Delta\phi = 1/(2\sqrt{\bar{n}})$, which is due to the shot-noise of the laser and for small $\bar{n}$ makes the measurement noisy. This can be overcome by increasing the read-out intensity. However, increasing the laser power also increases another noise source, namely the shot-noise induced backaction of the laser, which is just the uncertainty in the photon number $\Delta n = \sqrt{\bar{n}}$ of the laser. This results in random

"kicks" of the mechanical oscillator, which is proportional to $2\hbar k \sqrt{\bar{n}}$, and commonly called backaction noise. When increasing the read-out power the noise is first dominated by the phase uncertainty, while the backaction dominates at large powers. The point where the two contributions are of equal size is the so-called standard quantum limit (SQL), which for a position measurement of an oscillator with mass m and frequency ω_m is given by [84, 85]

$$\Delta x_{SQL} = \sqrt{\frac{\hbar}{2m\omega_m}}. \tag{2.77}$$

In all optomechanical experiments to date either the phase noise or the thermal noise dominate the backaction noise, and therefore it remains an outstanding goal to observe the backaction effects of radiation pressure (for a review on the quantum noise in measurements see [3]). Note that several schemes exist to circumvent this measurement limit by, for example, measuring only one quadrature of the resonator in a backaction evading scheme [86–88].[2]

2.3.5 Strong Coupling

In our experimental arrangement, the optomechanical system comprises two harmonic oscillators in the linearized regime, namely the light field and the mechanical resonator. In Sect. 2.1.1 we have seen that two coupled oscillators exhibit normal modes, which are non-degenerate in energy if their coupling exceeds the damping rates of the individual systems. This so-called strong coupling regime is interesting for optomechanical systems as coherent quantum control of the mechanical oscillator requires an energy exchange between the optical and the mechanical part that is faster than the dissipation rates of the two systems into their local environments, i.e. $g \gtrsim \kappa, \gamma_m$. This condition is also known from cavity QED [89] and solid state qubits coupled to photons [90, 91]. The normal mode splitting can be used as unambiguous evidence that the system actually is in the strong coupling regime, while the modes stay degenerate if g is small. As we have seen in Sect. 2.3.2 the optomechanical coupling can be increased by increasing the intra-cavity amplitude α_s, which experimentally corresponds to increasing the input laser power P.

In this section we will use a quantum approach to briefly derive the normal modes for the coupled optomechanical system and show that the splitting can only be observed when entering the strong coupling regime. The derivation and figures in this section are taken from the Supplementary Information of *Observation of strong coupling between a micromechanical resonator and an optical cavity field*, Nature **460**, 724–727 (2009) [46].

---

[2] Note that in the experiment presented in Sect. 5.2 we have achieved sub-SQL measurement precision [3].

We start by defining $\vec{R}^T = (x_c, p_c, x_m, p_m)$, where x and p are the amplitude (position) and phase (momentum) operators for the cavity field (the mechanical mode), respectively, and express the linearized Hamiltonian as $H = \frac{\hbar}{2} \vec{R}^T M \vec{R}$ where

$$
M = \begin{pmatrix} \Delta & 0 & g & 0 \\ 0 & \Delta & 0 & 0 \\ g & 0 & \omega_m & 0 \\ 0 & 0 & 0 & \omega_m \end{pmatrix}.
$$

The transformation to normal modes $\vec{R}^{NM} = (x_+, p_+, x_-, p_-)$ is achieved with a linear transformation $\vec{R}^{NM} = S\vec{R}$, where S fulfills $M = S^T \operatorname{diag}(\omega_+, \omega_+, \omega_-, \omega_-)S$ and is symplectic, i.e. it obeys $J = SJS^T$ where

$$
J = \begin{pmatrix} 0 & 1 & 0 & 0 \\ -1 & 0 & 0 & 0 \\ 0 & 0 & 0 & 1 \\ 0 & 0 & -1 & 0 \end{pmatrix}.
$$

The latter property guarantees that canonical commutation relations are conserved, i.e. $[\vec{R}_i, \vec{R}_j] = [\vec{R}_i^{NM}, \vec{R}_j^{NM}] = iJ_{ij}$. The explicit form of S can in principle be determined, but is quite involved and does not give much insight. As will become clear in a moment, the normal mode frequencies $\omega_\pm$ can be easily calculated without constructing S and are (in the absence of damping) given by

$$
\omega_\pm^2 = \frac{1}{2} \left(\Delta^2 + \omega_m^2 \pm \sqrt{(\Delta^2 - \omega_m^2)^2 + 4g^2 \omega_m \Delta} \right). \tag{2.78}
$$

The canonical operators evolve according to

$$
\dot{\vec{R}}(t) = i[H, \vec{R}(t)] - D\vec{R}(t) - \sqrt{2D}\vec{R}_{in}(t) = (JM - D)\vec{R}(t) - \sqrt{2D}\vec{R}_{in}(t), \tag{2.79}
$$

where we included damping of the cavity field and the mechanical resonator with $D = \operatorname{diag}(\kappa, \kappa, \gamma_m, \gamma_m)$ and Langevin forces $\vec{R}_{in}(t) = (x_{in}, p_{in}, f_{x_m}, f_{p_m})$. For white vacuum noise input to the cavity and a thermal white noise bath coupling to the mechanical system, all first moments vanish $\langle \vec{R}(t) \rangle \equiv 0$ and the only non-zero time correlation functions are

$$
\langle x_{in}(t) x_{in}(t') \rangle = \langle p_{in}(t) p_{in}(t') \rangle = \frac{1}{2}\delta(t - t'),
$$

$$
\langle f_{x_m}(t) f_{x_m}(t') \rangle = \langle f_{p_m}(t) f_{p_m}(t') \rangle = \left(\bar{n} + \frac{1}{2} \right)\delta(t - t'), \tag{2.80}
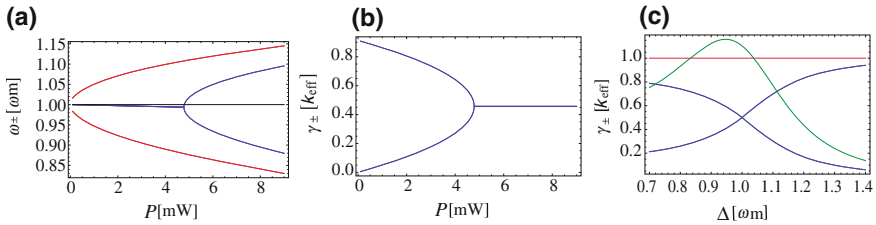$$

where $\bar{n} \approx \frac{k_B T}{\hbar \omega_m}$.

From (2.79) it is clear that eigenfrequencies and effective damping rates of the system are given by, respectively, the imaginary and real parts of the eigenvalues of $i(JM - D)$. The eigenvalues occur in complex conjugate pairs and the imaginary parts of the ones in the upper half plane determine eigenfrequencies. For the undamped system, $D = 0$, the eigenvalues are purely complex and one arrives at expression (2.78) for the normal mode frequencies. For the damped system, $D \neq 0$, the eigenvalues of $i(JM - D)$ will in general be complex and thus determine normal mode frequencies $\omega_\pm$ and effective damping rates $\gamma_\pm$ of normal modes, as exemplified in Fig. 2.7. While normal mode splitting (NMS) occurs for any non-zero coupling g in an undamped, a threshold of $g \gtrsim \kappa$ must be surpassed to observe NMS in a damped system [80, 92]. The effective damping rates behave complementary and merge above the same threshold. Comparison of the normal mode damping rates $\gamma_\pm$ to the effective mechanical damping rate (2.71) shows that the condition for resolving the normal mode peaks is $g \gg \kappa, \gamma_m$.

In terms of normal mode operators the full linearized Hamiltonian (2.75) is given by $H = \frac{\hbar\omega_+}{2}(x_+^2 + p_+^2) + \frac{\hbar\omega_-}{2}(x_-^2 + p_-^2)$. It can be expressed also in terms of creation and annihilation operators $a_\pm = (x_\pm + ip_\pm)/\sqrt{2}$ as $H = \hbar\omega_+\left(a_+^\dagger a_+ + \frac{1}{2}\right) + \hbar\omega_-\left(a_-^\dagger a_- + \frac{1}{2}\right)$. The Eigenstates and -energies are thus $H|n, m\rangle = E_{n,m}|n, m\rangle$, where

$$|n, m\rangle = \frac{1}{\sqrt{n!m!}}(a_+^\dagger)^n(a_-^\dagger)^m|0, 0\rangle,$$

$$E_{n,m} = \hbar\omega_+\left(n + \frac{1}{2}\right) + \hbar\omega_-\left(m + \frac{1}{2}\right). \tag{2.81}$$

Fig. 2.7 **a** Normal mode frequencies $\omega_\pm$ for an undamped (*red*) and a damped system (*blue*) for varying power of the driving laser. **b** Same for effective normal mode damping $\gamma_\pm$. **c** Effective damping rates of normal modes (*blue*), cavity amplitude decay rate κ (*red*) and effective mechanical decay rate γ_{eff} (*green*) for varying detuning. Not shown is the natural mechanical damping rate as $\gamma_m/\kappa \simeq 10^{-3}$. Parameters are as in Chap. 6, $\omega_m = 2\pi \times 947\,\text{kHz}$, $\gamma_m = 2\pi \times 140\,\text{Hz}$, $m_{eff} = 145\,\text{ng}$, $L = 25\,\text{mm}$, $\omega_c = 1.77 \times 10^{15}\,\text{Hz}$, $\kappa' = 2\pi \times 172\,\text{kHz}$ and $\bar{\kappa} = 2\pi \times 43\,\text{kHz}$. In **a** and **b** $\Delta = \omega_m$ and in **c** $P = 10.7\,\text{mW}$. Thanks to Klemens Hammerer for providing the plots

Emission of a cavity photon is in general accompanied by a transition of the optome-chanical system from one eigenstate to another by changing a single excitation, $|n, m\rangle \leftrightarrow |n - 1, m\rangle$ and $|n, m\rangle \leftrightarrow |n, m - 1\rangle$. In order for such a transi-tion to be allowed, the matrix element $\langle k, l|a_c|n, m\rangle$ must be non-zero, where $a_c = (x_c + ip_c)/\sqrt{2}$ is the annihilation operator for a cavity photon. From the linear relation $\vec{R} = S^{-1}\vec{R}^{NM}$ it is clear that a_c can be related to the normal mode creation and annihilation operators via a Bogoliubov transformation $a_c = \eta_1 a_+ + \eta_2 a_+^\dagger + \eta_3 a_- + \eta_4 a_-^\dagger$ where η_i are complex numbers. The energy splitting between these states is $E_{n,m} - E_{n-1,m} = \hbar\omega_+$ and $E_{n,m} - E_{n,m-1} = \hbar\omega_-$ respectively. Photons emitted from the cavity have to carry away this energy excess/deficiency relative to the incoming laser photons of frequency ω_l, i.e. they have to have frequencies $\omega_l \pm \omega_+$ or $\omega_l \pm \omega_-$.

The power spectral density of light emitted by the cavity is explicitly determined as follows: In frequency space $[\vec{R}(\omega) = \int d\omega \vec{R}(t) \exp(i\omega t)/\sqrt{2\pi}]$ the steady state solutions to the equations of motion (2.79) are

$$\vec{R}(\omega) = \frac{1}{i\omega + JM - D}\sqrt{2D}\vec{R}_{in}(\omega). \tag{2.82}$$

With the quantum optical cavity input-output relations (see for example [93, 94]) it follows that

$$\vec{R}_{out}(\omega) = \sqrt{2D}\vec{R}(\omega) + \vec{R}_{in}(\omega) = \left(\sqrt{2D}\frac{1}{i\omega + JM - D}\sqrt{2D} + 1\right)\vec{R}_{in}(\omega),$$

where $\vec{R}_{out}(\omega) = (x_{out}, p_{out}, f_{x_m,out}, f_{p_m,out})$. (x_{out}, p_{out}) are quadratures for the cavity output field which are subject to homodyne detection (see Sect. 3.6). In order to calculate their stationary properties we formally introduce also "phononic output fields" $(f_{x_m,out}, f_{p_m,out})$. The spectral correlation functions can be collected in a Hermitian spectral 4×4 correlation matrix $\gamma_{ij}^{out}(\omega, \omega') = \langle(\vec{R}_{out}(\omega'))_i(\vec{R}_{out}(\omega))_j\rangle$. Straight forward calculation yields $\gamma^{out}(\omega, \omega') = \delta(\omega + \omega')\Gamma(\omega)$ where

$$\Gamma(\omega) = \left(\sqrt{2D}\frac{1}{i\omega + JM - D}\sqrt{2D} + 1\right)N\left(\sqrt{2D}\frac{1}{-i\omega + JM - D}\sqrt{2D} + 1\right)^T$$

and $N = \text{diag}\left(\frac{1}{2}, \frac{1}{2}, \bar{n} + \frac{1}{2}, \bar{n} + \frac{1}{2}\right)$. The generalization of $\Gamma(\omega)$ where a lossy second mirror with an associated $\bar{\kappa}$ is taken into account can be found in [46]. Finally, the spectral density $S(\omega)$ is defined as $S(\omega)\delta(\omega + \omega') = \langle a_{out}^\dagger(\omega')a_{out}(\omega)\rangle$ where the amplitude operator for the cavity output field is $a_{out}(\omega) = (x_{out}(\omega) + ip_{out}(\omega))\sqrt{2}$. It follows from the definition of the spectral correlation matrix given above that

$$S(\omega) = \frac{1}{2}\left[\Gamma_{11}(\omega) + \Gamma_{22}(\omega) + i(\Gamma_{12}(\omega) - \Gamma_{21}(\omega))\right].$$

This expression gives the spectral density of sideband modes at a frequency $\omega_l + \omega$. In homodyne detection of sideband modes we do not distinguish sideband frequencies $\omega_l \pm \omega$ and extract only the overall noise power spectrum at a sideband frequency $|\omega|$, which is given by $S_{NPS}(\omega) = \sqrt{S(\omega)^2 + S(-\omega)^2}$. The calculated positions of the spectral peaks are in excellent agreement with measured data presented in Chap. 6.

2.3.6 Optomechanical Entanglement

The generation of entanglement between an optical light field and a mechanical oscillator is a major outstanding goal in the field of quantum opto-mechanics. Showing quantum entanglement with a massive macroscopic object is a sufficient condition for unambiguously demonstrating that quantum physics remains valid even for macroscopic systems. Besides the purely academic benefit of generating optomechanical entanglement and using it for generating non-classical mechanical states [31, 95], it is also at the heart of several applications in quantum information processing, such as quantum teleportation [96–98].

In quantum optics the generation of entangled states between two optical modes can nowadays be routinely achieved both for continuous variables [99] and discrete quantum systems [100]. The most commonly used technique to create an entangled state is to use down-conversion in a nonlinear medium. It is interesting to note, that the interaction of an optical field with the mechanical motion of an oscillator inside an optical cavity is also of a nonlinear nature, in fact part of it is the exact analogue to the down-conversion interaction in quantum optics. In the quantum optical continuous variable approach the resulting quantum states of the down-conversion process are 2-mode squeezed fields—exactly the same is produced if we pump the optical cavity in the optomechanical setup with a blue-detuned beam, only this time 2-mode squeezing between an optical and a mechanical continuous variable system is generated. For large squeezing the 2-mode squeezed states approximate the perfect correlations between conjugate observables as are required for an entangled state of the type described in the seminal paper by Einstein, Podolsky and Rosen (EPR) [101].

Let us first recall the situation for two optical modes. In simple conceptual terms the down-conversion (2-mode squeezing) interaction in a non-linear medium couples two previously uncorrelated modes via a Hamiltonian

$$H_{dc} = -i\hbar\chi(a_1^\dagger a_2^\dagger - a_1 a_2), \tag{2.83}$$

where $\chi \propto |\alpha_p|^2$ is the coupling strength between the optical modes 1, 2 and α_p is the amplitude of the optical pump field [99, 102, 103]. The main action of this interaction is to correlate one pair of quadratures between the outgoing modes, say the amplitude quadratures $x_{1,2} = (a_{1,2} + a_{1,2}^\dagger)/\sqrt{2}$, and anti-correlate the conjugate pair of quadratures, here the phase quadratures $p_{1,2} = (a_{1,2} - a_{1,2}^\dagger)/\sqrt{2}i$. With increasing

interaction strength the uncertainty in the sum (difference) between the quadratures decreases, $\Delta(x_1 - x_2)^2$, $\Delta(p_1 + p_2)^2 \to 0$, whereas the uncertainty in the individual quadrature increases. In the limiting case of infinite squeezing of these variances the two modes will eventually approximate the entangled state underlying the famous EPR argument [101], $|\Psi\rangle = \int dx |x, x\rangle = \int dp |p, -p\rangle = \sum_n |n, n\rangle$ (written here in position, momentum and number state representation, respectively). Realizations of sources for EPR entangled light, such as an optical parametric oscillator, typically require a cavity containing the nonlinear medium and supporting both modes 1 and 2. The EPR correlations between the modes can then be observed by performing two independent homodyne detections of light coupled out of these two cavities. The respective photocurrents for a given local oscillator phase ϕ_j ($j = 1, 2$) essentially provide a measurement of $x_j(\phi_j) = (a_j e^{i\phi_j} + \text{h.c.})/\sqrt{2}$. Cross correlating the two photocurrents thus constitutes a measurement of the correlations $\langle x_1(\phi_1) x_2(\phi_2) \rangle$, and scanning the local oscillator phases ϕ_j gives direct access to the quadrature correlations and anti-correlations characteristic of an EPR state. This way it was possible to realize the EPR paradox [99] and to use this entanglement for quantum teleportation [104].

Let us now draw the direct analogy to the optomechanical case. The radiation-pressure interaction between a mechanical oscillator with resonance frequency ω_m and an optical cavity field can effectively be described by (2.75)

$$H_{rp} = \hbar g(ab^\dagger + a^\dagger b) + \hbar g(ab + a^\dagger b^\dagger), \tag{2.84}$$

where the full Hamiltonian of the system is $H = H_0 + H_{rp}$ given by (2.60). The first term in the interaction H_{rp} describes the exchange of energy between the mechanical oscillator and the cavity field. As long as photons can leave the cavity this leads to (optical) cooling of the mechanical mode [38–40, 106]. The second term is the 2-mode squeezing, or down-conversion interaction, and stands for creation and annihilation of phonons and photons in pairs. Up to a change in phase it is equivalent to H_{dc} in Eq. (2.83). By choosing the detuning Δ of the laser from cavity resonance to be either $+\omega_m$ or $-\omega_m$ the first or the second process becomes resonant, respectively. The latter case resembles the desired down-conversion interaction H_{dc} between an optical cavity mode and a mechanical resonator mode, cf. Fig. 2.8b.

We focus on the situation where $\Delta \approx \omega_m$. In this case the so-called co-rotating (cooling) terms $ab^\dagger + a^\dagger b$ dominate the interaction while the so-called counter-rotating (down-conversion) terms $ab + a^\dagger b^\dagger$ contribute on the order of $\frac{g}{\omega_m}$, as can be directly seen from first-order perturbation theory. As long as the coupling strength is small, i.e. for $g \ll \omega_m$, one can neglect the counter-rotating terms and obtains the rotating wave approximation where only co-rotating terms are kept in the Hamiltonian [107]. This means that only cooling of the mechanical mode occurs (whose quantum limit is ultimately given exactly by the effects of counter-rotating terms). For increasing coupling strength, however, i.e. for $\frac{g}{\omega_m} \approx \mathcal{O}(1)$, this approximation is no longer valid and the regime beyond the rotating wave approximation becomes accessible. Specifically, while the co-rotating interaction increases its cooling action and hence prepares a mechanical input state of increasingly higher purity
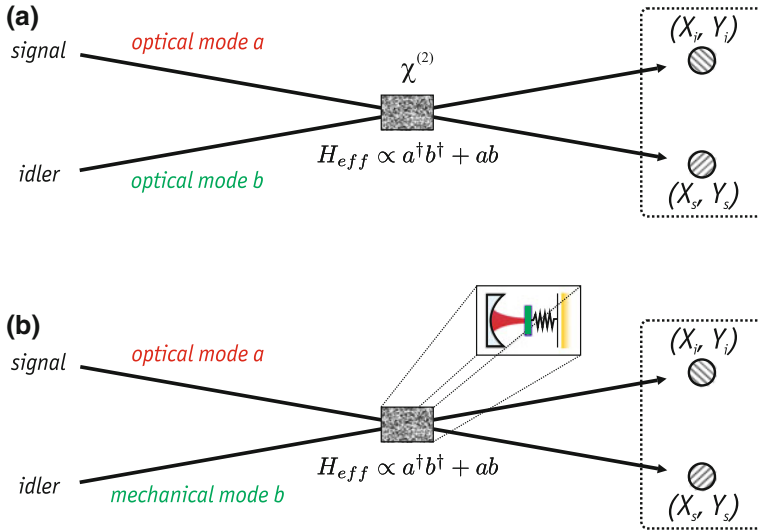
Fig. 2.8 a Down-conversion in continuous variable quantum optics. Two optical fields (signal and idler) interact in a nonlinear $\chi^{(2)}$ medium generating a 2-mode squeezed output state. The quadratures $X_{s,i}$ and $Y_{s,i}$ of the fields become non-classically correlated (figure adapted from Ou et al. [99]). **b** The optomechanical analogue to down-conversion—here the signal is an optical field non-linearly interacting with the vibrations of a mechanical resonator inside a properly detuned optical cavity. The effective interaction Hamiltonians of both **a** and **b** are equivalent. For properly chosen parameters (see text and Fig. 2.9) the optomechanical system becomes entangled and hence also exhibits non-classical correlations
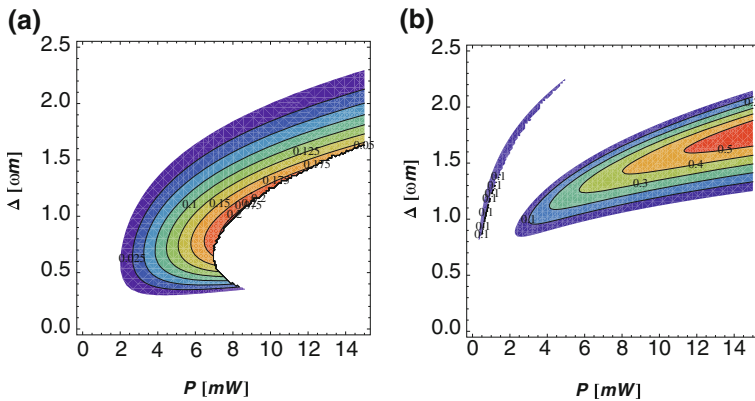
Fig. 2.9 Optomechanical entanglement. The entanglement measure plotted here is the logarithmic negativity E_N (for a definition see for example [105]) as a function of optical detuning Δ and input power P. Positive values of E_N mean that the optical and the mechanical systems are entangled. **a** The parameters are $\omega_m = 950$ kHz, $m_{eff} = 50$ ng, $Q = 30{,}000$, $L = 10$ mm, $F = 7{,}000$ and $T = 100$ mK. The maximal value of E_N is 0.2. **b** For this plot we chose $\omega_m = 360$ kHz, $m_{eff} = 50$ ng, $Q = 63{,}000$, $L = 25$ mm, $F = 14{,}000$ and $T = 100$ mK. We find a maximal E_N of 0.5. Note that the color coding of the contour plots is different for **a** and **b**. White areas mean that no entanglement is present. Thanks to Sebastian Hofer for providing the plots

(i.e. smaller entropy), the strength of the counter-rotating interaction also increases and enables optomechanical down-conversion to take place. Note that in the realm of atomic physics the rotating wave approximation is so good that there are only few demonstrations of physical effects that are due to counter-rotating terms [108]. In our experiment (see Chap. 7) it is the explicit breakdown of the rotating wave approximation that will allow us to combine state preparation with the desired nonlinear 2-mode interaction in a simple way (Fig. 2.9).

References

1. L. Bergmann, C. Schaefer, *Lehrbuch der Experimentalphysik: Band 1—Mechanik Relativität, Wärme* (de Gruyter, New York, 1998)
2. L.D. Landau, E.M. Lifshitz, *Mechanics*, 3rd edn. (Butterworth-Heinemann, London, 1976)
3. A.A. Clerk, M.H. Devoret, S.M. Girvin, F. Marquardt, R.J. Schoelkopf, Introduction to quantum noise, measurement, and amplification. Rev. Mod. Phys. **82**, 1155 (2010)
4. G. Breitenbach, *Quantum state reconstruction of classical and nonclassical light and a cryogenic opto-mechanical sensor for high-precision interferometry*, Ph.D. thesis, Universität Konstanz (1998)
5. R. Givens, O.F. de Alcantara Bonfim, R.B. Ormond, Direct observation of normal modes in coupled oscillators. Am. J. Phys. **71**, 87 (2003)
6. E. Schrödinger, Der stetige Übergang von der Mikro- zur Makromechanik. Naturwissenschaften **14**, 664 (1926)
7. R.J. Glauber, Coherent and incoherent states of the radiation field. Phys. Rev. **131**, 2766 (1963)
8. H.-A. Bachor, T.C. Ralph, *A Guide to Experiments in Quantum Optics*, 2nd edn. (Wiley-VCH, Weinheim, 2004)
9. E. Wigner, On the quantum correction for thermodynamic equilibrium. Phys. Rev. **40**, 749 (1932)
10. R.W. Spekkens, Negativity and contextuality are equivalent notions of nonclassicality. Phys. Rev. Lett. **101**, 020401 (2009)
11. M. Hillery, R.F. O'Connell, M.O. Scully, E.P. Wigner, Distribution functions in physics: fundamentals. Phys. Rep. **106**, 121 (1984)
12. J. Kepler, Letter to Galileo Galilei (1610)
13. J. Kepler, *De Cometis Libelli Tres* (Augsburg, Augustae Vindelicorum, 1619)
14. P. Lebedev, Untersuchungen über die Druckkräfte des Lichtes. Ann. Phys. **6**, 433 (1901)
15. E.F. Nichols, G.F. Hull, About radiation pressure. Ann. Phys. **12**, 225 (1903)
16. J.C. Maxwell, *A treatise on electricity and magnetism*, vol. 2 (Clarendon Press, Oxford, 1873)
17. A.G. Bartoli, *Sopra i movimenti prodotti dalla luce e dal calore e sopra il radiometro di Crookes* (Le Monnier, Florence, 1876)
18. V.B. Braginsky, Zh. Eksp. Teor. Fiz. **53**, 1434 (1967)
19. V.B. Braginsky, Y.I. Vorontsov, Quantum-mechanical limitations in macroscopic experiments and modern experimental technique. Sov. Phys. Usp. **17**, 644 (1975)
20. V. Braginsky, A. Manukin, *Measurement of Weak Forces in Physics Experiments* (University of Chicago Press, Chicago, 1977)
21. C.M. Caves, Quantum-mechanical radiation-pressure fluctuations in an interferometer. Phys. Rev. Lett. **45**, 75 (1980)
22. P. Meystre, E.M. Wright, J.D. McCullen, E. Vignes, Theory of radiation-pressure-driven interferometers. J. Opt. Soc. Am. B **2**, 1830 (1985)
23. A. Dorsel, J. McCullen, P. Meystre, E. Vignes, H. Walther, Optical bistability and mirror confinement induced by radiation pressure. Phys. Rev. Lett. **51**, 1550 (1983)

24. C. Fabre, M. Pinard, S. Bourzeix, A. Heidmann, E. Giacobino, S. Reynaud, Quantum-noise reduction using a cavity with a movable mirror. Phys. Rev. A **49**, 1337 (1994)
25. S. Mancini, P. Tombesi, Quantum noise reduction by radiation pressure. Phys. Rev. A **49**, 4055 (1994)
26. K. Jacobs, P. Tombesi, M.J. Collett, D.F. Walls, Quantum-nondemolition measurement of photon number using radiation pressure. Phys. Rev. A **49**, 1961 (1994)
27. M. Pinard, C. Fabre, A. Heidmann, Quantum-nondemolition measurement of light by a piezo-electric crystal. Phys. Rev. A **51**, 2443 (1995)
28. S. Mancini, D. Vitali, P. Tombesi, Optomechanical cooling of a macroscopic oscillator by homodyne feedback. Phys. Rev. Lett. **80**, 688 (1998)
29. P.-F. Cohadon, A. Heidmann, M. Pinard, Cooling of a mirror by radiation pressure. Phys. Rev. Lett. **83**, 3174 (1999)
30. S. Mancini, V.I. Man'ko, P. Tombesi, Ponderomotive control of quantum macroscopic coherence. Phys. Rev. A **55**, 3042 (1997)
31. S. Bose, K. Jacobs, P.L. Knight, Preparation of nonclassical states in cavities with a moving mirror. Phys. Rev. A **56**, 4175 (1997)
32. W. Marshall, C. Simon, R. Penrose, D. Bouwmeester, Towards quantum superpositions of a mirror. Phys. Rev. Lett. **91**, 130401 (2003)
33. J. Zhang, K. Peng, S.L. Braunstein, Quantum-state transfer from light to macroscopic oscillators. Phys. Rev. A **68**, 013808 (2003)
34. I. Tittonen, G. Breitenbach, T. Kalkbrenner, T. Müller, R. Conradt, S. Schiller, E. Steinsland, N. Blanc, N.F. de Rooij, Interferometric measurements of the position of a macroscopic body: towards observation of quantum limits. Phys. Rev. A **59**, 1038 (1999)
35. T. Briant, P. Cohadon, M. Pinard, A. Heidmann, Optical phase-space reconstruction of mirror motion at the attometer level. Eur. Phys. J. D **22**, 131 (2003)
36. O. Arcizet, P.-F. Cohadon, T. Briant, M. Pinard, A. Heidmann, J.-M. Mackowski, C. Michel, L. Pinard, O. François, L. Rousseau, High-sensitivity optical monitoring of a micro-mechanical resonator with a quantum-limited optomechanical sensor. Phys. Rev. Lett. **97**, 133601 (2006)
37. T. Kippenberg, H. Rokhsari, T. Carmon, A. Scherer, K. Vahala, Analysis of radiation-pressure induced mechanical oscillation of an optical microcavity. Phys. Rev. Lett. **95**, 033901 (2005)
38. S. Gigan, H.R. Böhm, M. Paternostro, F. Blaser, G. Langer, J.B. Hertzberg, K.C. Schwab, D. Bäuerle, M. Aspelmeyer, A. Zeilinger, Self-cooling of a micromirror by radiation pressure. Nature **444**, 67 (2006)
39. O. Arcizet, P.-F. Cohadon, T. Briant, M. Pinard, A. Heidmann, Radiation-pressure cooling and optomechanical instability of a micromirror. Nature **444**, 71 (2006)
40. A. Schliesser, P. Del'Haye, N. Nooshi, K.J. Vahala, T.J. Kippenberg, Radiation pressure cooling of a micromechanical oscillator using dynamical backaction. Phys. Rev. Lett. **97**, 243905 (2006)
41. T. Corbitt, Y. Chen, E. Innerhofer, H. Müller-Ebhardt, D. Ottaway, H. Rehbein, D. Sigg, S. Whitcomb, C. Wipf, N. Mavalvala, An all-optical trap for a gram-scale mirror. Phys. Rev. Lett. **98**, 150802 (2007)
42. S. Gröblacher, S. Gigan, H.R. Böhm, A. Zeilinger, M. Aspelmeyer, Radiation-pressure self-cooling of a micromirror in a cryogenic environment. Europhys. Lett. **81**, 54003 (2008)
43. S. Gröblacher, J.B. Hertzberg, M.R. Vanner, S. Gigan, K.C. Schwab, M. Aspelmeyer, Demonstration of an ultracold micro-optomechanical oscillator in a cryogenic cavity. Nat. Phys. **5**, 485 (2009)
44. Y.-S. Park, H. Wang, Resolved-sideband and cryogenic cooling of an optomechanical resonator. Nat. Phys. **5**, 489 (2009)
45. A. Schliesser, O. Arcizet, R. Rivière, G. Anetsberger, T.J. Kippenberg, Resolved-sideband cooling and position measurement of a micromechanical oscillator close to the Heisenberg uncertainty limit. Nat. Phys. **5**, 509 (2009)
46. S. Gröblacher, K. Hammerer, M.R. Vanner, M. Aspelmeyer, Observation of strong coupling between a micromechanical resonator and an optical cavity field. Nature **460**, 724 (2009)

47. E. Verhagen, S. Deléglise, S. Weis, A. Schliesser, T.J. Kippenberg, Quantum-coherent coupling of a mechanical oscillator to an optical cavity mode. Nature **482**, 63 (2012)
48. E.F. Nichols, G.F. Hull, The pressure due to radiation. Proc. Am. Acad. Arts Sci. **38**, 559 (1903)
49. T.J. Kippenberg, K.J. Vahala, Cavity opto-mechanics. Opt. Express **15**, 17172 (2007)
50. M. Aspelmeyer, K.C. Schwab, Mechanical systems at the quantum limit. New J. Phys. **10**, 095001 (2008)
51. I. Favero, K. Karrai, Optomechanics of deformable optical cavities. Nat. Photon. **3**, 201 (2009)
52. F. Marquardt, S.M. Girvin, Optomechanics. Physics **2**, 40 (2009)
53. C. Genes, A. Mari, D. Vitali, P. Tombesi, Quantum effects in optomechanical systems. Adv. At. Mol. Opt. Phys. **57**, 33 (2009)
54. M. Aspelmeyer, S. Gröblacher, K. Hammerer, N. Kiesel, Quantum optomechanics— throwing a glance. J. Opt. Soc. Am. B **27**, A189 (2010)
55. A. Naik, O. Buu, M.D. LaHaye, A.D. Armour, A.A. Clerk, M.P. Blencowe, K.C. Schwab, Cooling a nanomechanical resonator with quantum back-action. Nature **443**, 193 (2006)
56. C.A. Regal, J.D. Teufel, K.W. Lehnert, Measuring nanomechanical motion with a microwave cavity interferometer. Nat. Phys. **4**, 555 (2008)
57. J.D. Teufel, J.W. Harlow, C.A. Regal, K.W. Lehnert, Dynamical backaction of microwave fields on a nanomechanical oscillator. Phys. Rev. Lett. **101**, 197203 (2008)
58. T. Rocheleau, T. Ndukum, C. Macklin, J.B. Hertzberg, A.A. Clerk, K.C. Schwab, Preparation and detection of a mechanical resonator near the ground state of motion. Nature **463**, 72 (2010)
59. J.D. Teufel, D. Li, M.S. Allman, K. Cicak, A.J. Sirois, J.D. Whittaker, R.W. Simmonds, Circuit cavity electromechanics in the strong-coupling regime. Nature **471**, 204 (2011)
60. A.H. Safavi-Naeini, J. Chan, J.T. Hill, T.P.M. Alegre, A. Krause, O. Painter, Observation of quantum motion of a nanomechanical resonator. Phys. Rev. Lett. **108**, 033602 (2012)
61. A.D. O'Connell, M. Hofheinz, M. Ansmann, R.C. Bialczak, M. Lenander, E. Lucero, M. Neeley, D. Sank, H. Wang, M. Weides, J. Wenner, J.M. Martinis, A.N. Cleland, Quantum ground state and single-phonon control of a mechanical resonator. Nature **464**, 697 (2010)
62. J.D. Jost, J.P. Home, J.M. Amini, D. Hanneke, R. Ozeri, C. Langer, J.J. Bollinger, D. Leibfried, D.J. Wineland, Entangled mechanical oscillators. Nature **459**, 683 (2009)
63. J. Kerr, On a new relation between electricity and light: dielectric media birefringent. Phil. Mag. **1**, 337 (1875)
64. D.J. Wineland, W.M. Itano, Laser cooling of atoms. Phys. Rev. A **20**, 1521 (1979)
65. H.B. Callen, T.A. Welton, Irreversibility and generalized noise. Phys. Rev. **83**, 34 (1951)
66. M. Pinard, Y. Hadjar, A. Heidmann, Effective mass in quantum effects of radiation pressure. Eur. Phys. J. D **7**, 107 (1999)
67. M. Paternostro, S. Gigan, M.S. Kim, F. Blaser, H.R. Böhm, M. Aspelmeyer, Reconstructing the dynamics of a movable mirror in a detuned optical cavity. New J. Phys. **8**, 107 (2006)
68. C. Genes, D. Vitali, P. Tombesi, S. Gigan, M. Aspelmeyer, Ground-state cooling of a micro-mechanical oscillator: comparing cold damping and cavity-assisted cooling schemes. Phys. Rev. A **77**, 033804 (2008)
69. C.K. Law, Effective Hamiltonian for the radiation in a cavity with a moving mirror and a time-varying dielectric medium. Phys. Rev. A **49**, 433 (1994)
70. P. Langevin, Sur la théorie du mouvement brownien. C. R. Acad. Sci. **146**, 530 (1908)
71. W.T. Coffey, Y.P. Kalmykov, J.T. Waldron, *The Langevin Equation*, 2nd edn. (World Scientific Publishing, Singapore, 2004)
72. M. Vogel, C. Mooser, K. Karrai, R. Wartburton, Optically tunable mechanics of microlevers. Appl. Phys. Lett. **83**, 1337 (2003)
73. B. Sheard, M. Gray, C. Mow-Lowry, D. McClelland, Observation and characterization of an optical spring. Phys. Rev. A **69**, 051801 (2004)
74. T. Corbitt, D. Ottaway, E. Innerhofer, J. Pelc, N. Mavalvala, Measurement of radiation-pressure-induced optomechanical dynamics in a suspended Fabry-Perot cavity. Phys. Rev. A **74**, 021802 (2006)

75. A.D. Virgilio, L. Barsotti, S. Braccini, C. Bradaschia, G. Cella, C. Corda, V. Dattilo, I. Ferrante, F. Fidecaro, I. Fiori, F. Frasconi, A. Gennai, A. Giazotto, P.L. Penna, G. Losurdo, E. Majorana, M. Mantovani, A. Pasqualetti, D. Passuello, F. Piergiovanni, A. Porzio, P. Puppo, P. Rapagnani, F. Ricci, S. Solimeno, G. Vajente, F. Vetrano, Experimental evidence for an optical spring. Phys. Rev. A **74**, 013813 (2006)

76. T. Corbitt, C. Wipf, T. Bodiya, D. Ottaway, D. Sigg, N. Smith, S. Whitcomb, N. Mavalvala, Optical dilution and feedback cooling of a gram-scale oscillator to 6.9 mK. Phys. Rev. Lett. **99**, 160801 (2007)

77. L. Diósi, Laser linewidth hazard in optomechanical cooling, Phys. Rev. A **78**, 021801(R) (2008)

78. P. Rabl, C. Genes, K. Hammerer, M. Aspelmeyer, Phase-noise induced limitations on cooling and coherent evolution in optomechanical systems. Phys. Rev. A **80**, 063819 (2009)

79. I. Wilson-Rae, N. Nooshi, W. Zwerger, T.J. Kippenberg, Theory of ground state cooling of a mechanical oscillator using dynamical back-action. Phys. Rev. Lett. **99**, 093901 (2007)

80. F. Marquardt, J.P. Chen, A.A. Clerk, S.M. Girvin, Quantum theory of cavity-assisted sideband cooling of mechanical motion. Phys. Rev. Lett. **99**, 093902 (2007)

81. J.D. Thompson, B.M. Zwickl, A.M. Jayich, F. Marquardt, S.M. Girvin, J.G.E. Harris, Strong dispersive coupling of a high-finesse cavity to a micromechanical membrane. Nature **452**, 72 (2008)

82. J. Chan, T.P.M. Alegre, A.H. Safavi-Naeini, J.T. Hill, A. Krause, S. Gröblacher, M. Aspelmeyer, O. Painter, Laser cooling of a nanomechanical oscillator into its quantum ground state. Nature **478**, 89 (2011)

83. J.D. Teufel, T. Donner, D. Li, J.H. Harlow, M.S. Allman, K. Cicak, A.J. Sirois, J.D. Whittaker, K.W. Lehnert, R.W. Simmonds, Sideband cooling of micromechanical motion to the quantum ground state. Nature **475**, 359 (2011)

84. C.M. Caves, K.S. Thorne, R.W.P. Drever, V.D. Sandberg, M. Zimmermann, On the measurement of a weak classical force coupled to a quantum-mechanical oscillator. I. Issues of principle. Rev. Mod. Phys. **52**, 341 (1980)

85. V. Braginsky, F. Khalili, *Quantum Measurements* (Cambridge University Press, Cambridge, 1995)

86. V.B. Braginsky, Y.I. Vorontsov, K.S. Thorne, Quantum nondemolition measurements. Science **209**, 547 (1980)

87. A.A. Clerk, F. Marquardt, K. Jacobs, Back-action evasion and squeezing of a mechanical resonator using a cavity detector. New J. Phys. **10**, 095010 (2008)

88. J.B. Hertzberg, T. Rocheleau, T. Ndukum, M. Savva, A.A. Clerk, K.C. Schwab, Back-action-evading measurements of nanomechanical motion. Nat. Phys. **6**, 213 (2009)

89. H. Walther, B.T.H. Varcoe, B.-G. Englert, T. Becker, Cavity quantum electrodynamics. Rep. Prog. Phys. **69**, 1325 (2006)

90. A. Wallraff, D.I. Schuster, A. Blais, L. Frunzio, R.-S. Huang, J. Majer, S. Kumar, S.M. Girvin, R.J. Schoelkopf, Strong coupling of a single photon to a superconducting qubit using circuit quantum electrodynamics. Nature **431**, 162 (2004)

91. G. Khitrova, H.M. Gibbs, M. Kira, S.W. Koch, A. Scherer, Vacuum Rabi splitting in semiconductors. Nat. Phys. **2**, 81 (2006)

92. J.M. Dobrindt, I. Wilson-Rae, T.J. Kippenberg, Parametric normal-mode splitting in cavity optomechanics. Phys. Rev. Lett. **101**, 263602 (2008)

93. M.J. Collett, C.W. Gardiner, Squeezing of intracavity and traveling-wave light fields produced in parametric amplification. Phys. Rev. A **30**, 1386 (1984)

94. C.W. Gardiner, M.J. Collett, Input and output in damped quantum systems: quantum stochastic differential equations and the master equation. Phys. Rev. A **31**, 3761 (1985)

95. E. Schrödinger, Die gegenwärtige Situation in der Quantenmechanik. Die Naturwissenschaften **48**, 808 (1935)

96. C.H. Bennett, G. Brassard, C. Crépeau, R. Jozsa, A. Peres, W.K. Wootters, Teleporting an unknown quantum state via dual classical and Einstein-Podolsky-Rosen channels. Phys. Rev. Lett. **70**, 1895 (1993)

97. D. Bouwmeester, J.-W. Pan, K. Mattle, M. Eibl, H. Weinfurter, A. Zeilinger, Experimental quantum teleportation. Nature **390**, 575 (1997)
98. S.G. Hofer, W. Wieczorek, M. Aspelmeyer, K. Hammerer, Quantum entanglement and teleportation in pulsed cavity optomechanics. Phys. Rev. A **84**, 052327 (2011)
99. Z.Y. Ou, S.F. Pereira, H.J. Kimble, K.C. Peng, Realization of the Einstein-Podolsky-Rosen paradox for continuous variables. Phys. Rev. Lett. **68**, 3663 (1992)
100. P.G. Kwiat, K. Mattle, H. Weinfurter, A. Zeilinger, A.V. Sergienko, Y. Shih, New high-intensity source of polarization-entangled photon pairs. Phys. Rev. Lett. **75**, 4337 (1995)
101. A. Einstein, B. Podolsky, N. Rosen, Can quantum-mechanical description of physical reality be considered complete? Phys. Rev. **47**, 777 (1935)
102. S.L. Braunstein, P. van Loock, Quantum information with continuous variables. Rev. Mod. Phys. **77**, 513 (2005)
103. C. Simon, D. Bouwmeester, Theory of an entanglement laser. Phys. Rev. Lett. **91**, 053601 (2003)
104. A. Furusawa, J.L. Sörensen, S.L. Braunstein, C.A. Fuchs, H.J. Kimble, E.S. Polzik, Unconditional quantum teleportation, Science **282**, 706 (1998)
105. M.B. Plenio, Logarithmic negativity: a full entanglement monotone that is not convex. Phys. Rev. Lett. **95**, 090503 (2005)
106. V. Braginsky, S.P. Vyatchanin, Low quantum noise tranquilizer for Fabry-Perot interferometer. Phys. Lett. A **293**, 228 (2002)
107. P. Meystre, M. Sargent, *Elements of Quantum Optics* (Springer, Heidelberg, 1990)
108. S. Hofferberth, B. Fischer, T. Schumm, J. Schmiedmayer, I. Lesanovsky, Ultracold atoms in radio-frequency dressed potentials beyond the rotating-wave approximation. Phys. Rev. A **76**, 013401 (2007)